

Stimulated-Raman-scattering-assisted superfluorescence enhancement from ionized nitrogen molecules in 800-nm femtosecond laser fields

Zhiming Miao,¹ Xunqi Zhong,¹ Linlin Zhang,¹ Wei Zheng,¹ Yunan Gao,^{1,3} Yunquan Liu,^{1,2,3} Hongbing Jiang,^{1,3} Qihuang Gong,^{1,2,3} and Chengyin Wu^{1,2,3,*}

¹State Key Laboratory for Mesoscopic Physics, School of Physics, Peking University, Beijing 100871, China

²Collaborative Innovation Center of Quantum Matter, Beijing 100871, China

³Collaborative Innovation Center of Extreme Optics, Shanxi University, Taiyuan, Shanxi 030006, China



(Received 11 July 2018; published 4 September 2018)

We have observed collective spontaneous emission (superfluorescence) from ionized nitrogen molecules generated by 800-nm laser pulses. The superfluorescence intensity around 391 nm was found to be greatly enhanced when injecting an external seed with various wavelengths. Our finding provides insights into controlling the coherent emission from air filamentation induced by intense femtosecond laser fields, which has great potential application in remote atmospheric sensing.

DOI: [10.1103/PhysRevA.98.033402](https://doi.org/10.1103/PhysRevA.98.033402)

I. INTRODUCTION

Ultrashort and ultraintense bench-top lasers are available in laboratories due to the rapid development of laser technology, which greatly promotes the study of laser-matter interaction in the nonperturbative regime. Such laser-matter interaction provides other routes to manipulate both the laser and the matter [1–3]. Narrow-band coherent emissions around 471, 428, 391, 357, and 330 nm were observed by Yao *et al.* when they investigated the propagation of intense mid-infrared femtosecond laser pulses in air [4]. These emission lines have been assigned to the transitions between $N_2^+(B^2\Sigma_u^+, v' = 0 - 2)$ and $N_2^+(X^2\Sigma_g^+, v = 0 - 2)$. The observation shows that the nonperturbative interaction between intense mid-infrared laser fields and nitrogen molecules can be used to generate wavelength-tunable narrow-bandwidth coherent emission covering ultraviolet to visible wavelength region along the laser propagation direction. This directional emission utilizes the main constitutions of ambient air nitrogen as the gain medium and is also termed as air lasing. It improves tremendously the detection sensitivity of optical remote sensing in comparison with the nondirectional fluorescence.

Various schemes have been proposed for generating air lasing based on the understanding of laser-matter interaction [5–11]. However, the laser-molecule interaction is very complicated when the laser field becomes intensive [12]. Tunneling ionization is one of the fundamental processes for molecules in intense femtosecond laser fields. According to strong field molecular orbital theory [13], the molecular ions are in the ground electronic state when the electron in the highest occupied molecular orbital (HOMO) is removed. Therefore, the molecular ions are in the excited electronic states when ionization occurs through lower-lying orbitals.

Advanced experimental methods have been developed to identify the electronic states of molecular ions generated by intense femtosecond laser fields [14–18]. Because the ionization rate decays exponentially with respect to the electron binding energy, it is usually assumed that the molecular ion is dominantly in its ground electronic state. The generation of air lasing from ionized nitrogen molecules implies that excited electronic state plays a significant role in the laser filamentation [19]. It is even suggested that the population in the excited electronic state can be higher than that in the ground electronic state for ionized nitrogen molecules [20–22]. Evidence shows that the multiple coherent emission lines are generated from a series of nonlinear processes including four-wave mixing and stimulated-Raman scattering in the case of a mid-infrared driving laser field [23,24]. However, the underlying mechanism is still highly debated in the case of a 800-nm driving laser field [25–31].

Previous work has concentrated on measuring the intensity variation of the external seed based on the pump-probe technique, and it has been found that the intensity of the external seed can be either amplified or attenuated depending on the wavelength of the pump laser or the external seed [21,27]. In this paper, we found that the coherent emission around 391 nm can be greatly enhanced when an external seed around 357 nm is injected into the ionized nitrogen molecules generated by the 800-nm laser fields. By comparing the temporal profile and the intensity of the enhanced 391-nm emission induced by an external seed with different wavelengths, we concluded that the enhanced 391-nm emission originates from the seed-induced superfluorescence. In the case of the 357-nm seed, the 391-nm coherent emission is first generated by the stimulated vibrational Raman-scattering process, the generated 391-nm coherent emission then serves as an external seed to induce the superfluorescence from the ionized nitrogen molecules. This study demonstrates that the seed wavelength does not have to cover the lasing wavelength from ionized nitrogen molecules.

*cywu@pku.edu.cn

II. EXPERIMENTAL SETUP

The experiments were carried out using a commercial Ti:sapphire laser amplifier, which delivers linearly polarized femtosecond laser pulses with a central wavelength of 800 nm, pulse duration of 35 fs, and pulse energy of 6 mJ. The 800-nm laser beam was split into three beams by two beam splitters. The first 800-nm laser beam with a single pulse energy of about 2 mJ was utilized as a pump laser to ionize neutral nitrogen molecules. The second 800-nm laser beam with a single pulse energy of about 3 mJ was introduced into an optical parametric amplifier system to generate a tunable mid-infrared laser source. Its fourth harmonics was generated by two BBO crystals and utilized as an external seed. The third weak 800-nm laser beam was utilized to generate the sum frequency signal with the 391-nm coherent emission from ionized nitrogen molecules in a BBO crystal. In the experiment, the pump laser and the seed were recombined collinearly by a dichroic mirror with high reflectivity around 320–470 nm and high transmission around 680–900 nm. Then they were focused by an $f = 300$ mm convex lens into a gas chamber filled with pure nitrogen gas. After filtering the 800-nm pump laser by another pair of dichroic mirrors, the forward emission was focused into a fiber spectrometer. The intensity of the forward emission from ionized nitrogen molecules was measured as a function of the time delay between the 800-nm pump laser and the external seed. The temporal profile of the coherent emission was obtained by combining it with the third 800-nm laser beam to measure its sum frequency signal.

III. RESULTS AND DISCUSSION

Figure 1(a) shows a typical forward emission spectra from ionized nitrogen molecules generated by intense 800-nm laser fields. The incident laser was linearly polarized with pulse

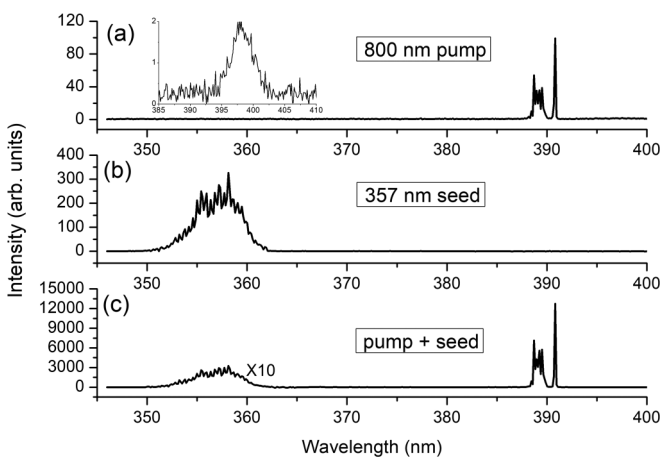


FIG. 1. (a) Forward emission of pure nitrogen molecules irradiated by intense 800-nm pump laser. In the inset the broad emission around 400 nm is generated in argon atoms and attributed to the second harmonic of the 800-nm pump laser. (b) Spectrum of the 357-nm external seed. (c) Forward emission in the presence of an external 357-nm seed with optimized time delay. The region around 357 nm is magnified by a factor of 10 for visual convenience.

energy of 1.5 mJ and the gas pressure was 10 mbar. The emission lines around 391 nm were assigned to the transition of a P-branch and around 388 nm they were assigned to an R-branch of $N_2^+(B^2\Sigma_u^+, v' = 0 \rightarrow X^2\Sigma_g^+, v = 0)$. In the inset a broad emission around 400 nm is clearly observed in argon atoms under a similar laser condition. The observation confirmed that the second harmonic can be generated by simply focusing an intense laser pulse in gases. It is known that the inversion symmetry is required to be broken for generating second harmonic generation in gases, which is realized by the charge separation induced by the intense laser fields [32]. In agreement with previous reports [33,34], the observed coherent emissions around 391 and 388 nm are attributed to the self-seed triggered lasing and the seed is served by the second harmonic of the pump laser. Fig. 1(b) shows the spectrum of an external seed around 357 nm. The 357-nm seed has a duration of about 200 fs and the wavelength corresponds to the transition of $(N_2^+B^2\Sigma_u^+, v' = 1 \rightarrow X^2\Sigma_g^+, v = 0)$. As shown in Fig. 1(c), the forward emission around 391 nm is greatly enhanced by more than two orders of magnitude when the 357-nm seed is injected with an optimized time delay between the pump laser and the seed. It should be emphasized that the absolute intensity of the enhanced 391-nm coherent emission is about 50 times of the seed laser intensity.

Figure 2(a) shows the enhanced 391-nm emission intensity as a function of the time delay between the 800-nm pump laser and the 357-nm seed. It can be seen that the enhancement occurs only in a limited temporal window near the duration of the 357-nm seed (200 fs). Further, we measured the sum frequency signal at 263 nm with a third weak 800-nm laser beam in a BBO crystal and obtained the temporal profile of the enhanced 391-nm emission. As shown in Fig. 2(b), the enhanced 391-nm coherent emission lags behind the 357-nm seed with a time of ~ 4 ps. In addition, the lagged emission lasts several tens of picoseconds and is superimposed by some periodic modulations. The interval of ~ 4 ps corresponds

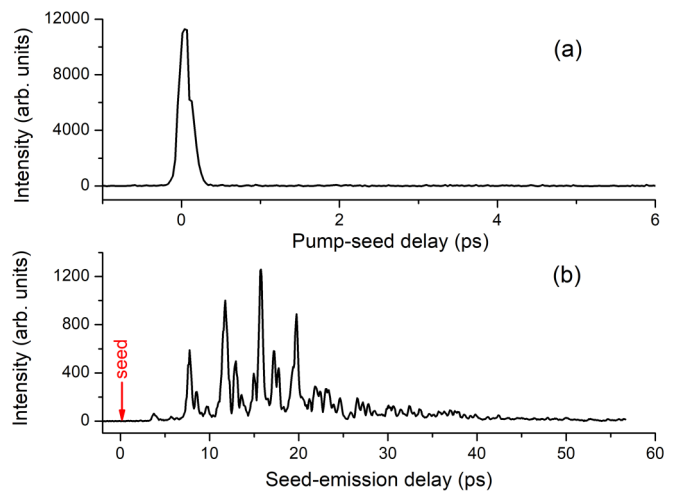


FIG. 2. (a) The intensity of the enhanced 391-nm emission as a function of time delay between the 800-nm pump laser and the 357-nm external seed; (b) the sum frequency signal at 263 nm generated by the enhanced 391-nm emission and the weak 800-nm laser as a function of time delay between them. The injection time of the external 357-nm seed is marked by a red arrow.

to the half fundamental rotational period of the rotational wave packet of $N_2^+(B^2\Sigma_u^+)$. The duration of the enhanced 391-nm emission (~ 40 ps) is more than two orders of magnitude longer than that of the 357-nm seed (200 fs). This measurement indicates that the enhanced 391-nm emission is not produced directly from parametric processes, in which temporal overlap is expected. It should be mentioned that, Li *et al.* [35] reported that the duration of the 391-nm coherent emission becomes shorter with increasing the plasma length and the emission signal shows oscillation depending on the plasma length. Liu *et al.* [19] measured the emission delay, pulse duration, and peak power of the 391-nm emission as a function of gas pressure. All results indicate that the 391-nm coherent emission shows the nature of superradiance. Here we noticed that the duration of the enhanced 391-nm emission is about three orders of magnitude shorter than the spontaneous lifetime of corresponding transition (~ 60 ns) in our experimental condition. The phenomena that the emission duration is several orders of magnitude shorter than its spontaneous lifetime has been observed in the $1s^2 \rightarrow 1s3p$ excitation of helium atoms by 53.7-nm free-electron laser radiation and the emission is attributed to a kind of collective spontaneous emission, i.e., superfluorescence [36]. Combining previous reports and the present measurement, the lagged 391-nm coherent emission in our experiment is attributed to the seed-induced superfluorescence. In comparison with atoms, the temporal profile of the superfluorescence is more complicated for molecules due to the molecular rotation and vibration.

In intense femtosecond laser fields, nitrogen molecules are ionized through tunneling process. At the moment of ionization, $N_2^+(B^2\Sigma_u^+)$ and $N_2^+(X^2\Sigma_g^+)$ are aligned along the polarization direction of the pump laser due to the anisotropic angular-dependent ionization probability [37]. After the laser pulse, the transient alignment is revived at the times of the integers of half rotational period of ionized nitrogen molecules. As shown in Fig. 1(c), the superfluorescence around 391 and 388 nm consists of many rotational emission lines corresponding to the P-branch and R-branch of $N_2^+(B^2\Sigma_u^+, v' = 0 \rightarrow X^2\Sigma_g^+, v = 0)$ transition. The dipole moment and emission polarization are parallel to the molecular axis for these transitions [21]. At the times corresponding to the integers of half rotational revival of ionized nitrogen molecules, all emission lines carry the same phase between different rotational states of $N_2^+(B^2\Sigma_u^+, v' = 0)$ and $N_2^+(X^2\Sigma_g^+, v = 0)$. The constructive interference leads to periodic modulation of the enhanced 391-nm emission at the times of the integers of half fundamental rotational period of the rotational wave packet of $N_2^+(B^2\Sigma_u^+)$, as shown in Fig. 2(b).

In order to reveal the underlying mechanism, we carried out similar experiments but using the seed with wavelength of 391 nm. As shown in Fig. 3(a), the enhanced 391-nm emission is also achieved in the presence of a 391-nm external seed. However, the absolute intensity of the 391-nm seed is much lower than that of the 357-nm seed to achieve the same intensity of the enhanced 391-nm emission under the same experimental condition (pump laser and gas pressure). Figure 3(b) shows the enhanced 391-nm signal as a function of the time delay between the pump laser and the seed. Different from the 357-nm seed, the enhancement of the 391-nm emission can occur in a broad time window of several

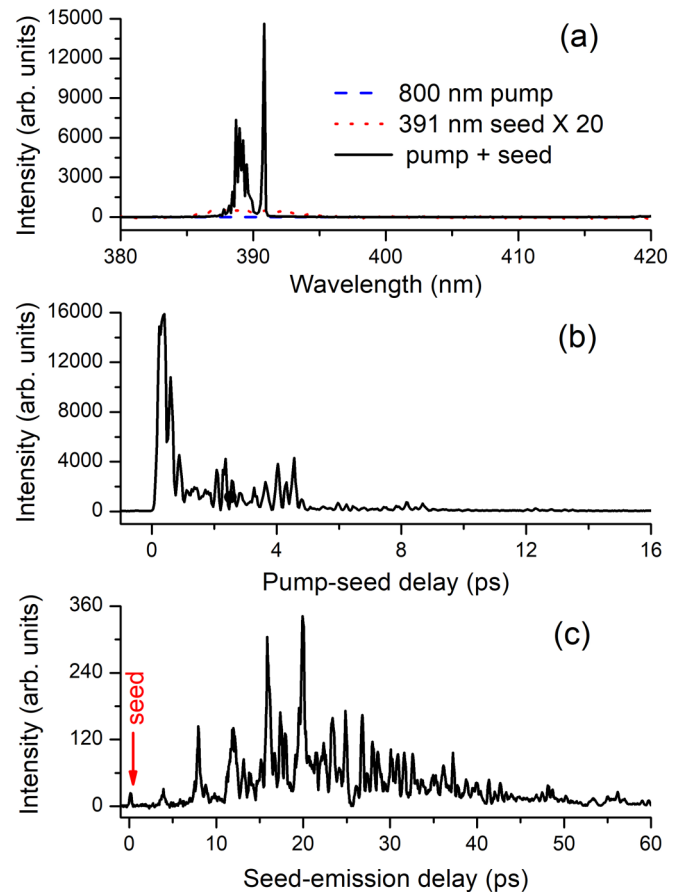


FIG. 3. (a) Forward emission in the presence of an external 391-nm seed with optimized time delay, the seed laser around 391 nm is magnified by a factor of 20 for visual convenience; (b) the intensity of the enhanced 391-nm emission as a function of time delay between the 800-nm pump laser and the 391-nm external seed; (c) the sum frequency signal at 263 nm generated by the enhanced 391-nm emission and the 800-nm laser as a function of time delay between them. The injection time of the external 391-nm seed is marked by a red arrow.

picoseconds when the 391-nm seed is applied. In addition, the time-dependent enhancement is superimposed by some periodic modulations. Figure 3(c) shows the temporal profile of the enhanced 391-nm emission by measuring the sum frequency signal at 263 nm with a weak 800-nm laser beam in a BBO crystal. The peak marked by a red arrow comes from the sum frequency signal of the external 391-nm seed and the weak 800-nm laser. This assignment is confirmed by blocking the 800-nm pump laser; the peak still exists and the intensity has no obvious change. This observation clearly demonstrates that the external seed itself is not directly amplified. The enhanced 391-nm emission lags behind the seed. The duration of the lagged 391-nm emission is tens of picoseconds. It is also superimposed by some periodic modulations separated by ~ 4 ps. All these features are similar to the case of 357-nm seed. The similarity indicates that the enhanced 391-nm emission is a kind of collective spontaneous emission (superfluorescence) whether the 357-nm or the 391-nm seed is applied.

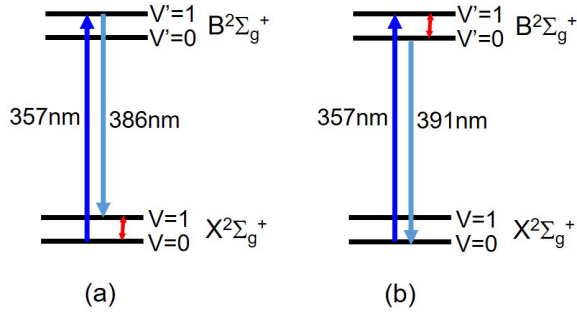


FIG. 4. Resonance enhanced Raman scattering related with vibrational Raman process from (a) $N_2^+(X^2\Sigma_g^+, v=0 \rightarrow v=1)$, and (b) $N_2^+(B^2\Sigma_u^+, v'=0 \rightarrow v'=1)$.

The main difference between two cases is that the enhancement of the 391-nm emission occurs in a limited time window (~ 200 fs) in the case of the 357-nm seed and a broad time window (~ 10 ps) in the case of the 391-nm seed. Macroscopic coherence is shown to be crucial for the 391-nm coherent emission [38]. The coherence is built through absorbing and emitting photons. The transition probability of the R branch depends on the phase of $2\pi c[B_B J(J+1) - B_x J(J-1)]t$ and the P branch on the phase of $2\pi c[B_B J(J+1) - B_x(J+1)(J+2)]t$, where J is the rotational quantum number of $N_2^+(B^2\Sigma_u^+, v'=0)$, B_B and B_x are the rotational constants of $N_2^+(B^2\Sigma_u^+, v'=0)$ and $N_2^+(X^2\Sigma_g^+, v=0)$, respectively. All rotational states were initially populated by the 800-nm pump laser and the time is set to zero at the moment of ionization. At the times corresponding to the integers of half rotational revival of ionized nitrogen molecules, all the transition experiences the same phase and the maximum coherence, as well as the maximum enhancement, is achieved. This result agrees well with the very recent report by Arissian *et al.* that the gain is strongly dependent on the phase [30]. Based on the comparative analysis of cases using a 357-nm and a 391-nm seed, we suggest the following mechanism for the enhanced 391-nm emission induced by the 357-nm seed. When a 357-nm seed is injected into the ionized nitrogen molecules, a coherent emission around ~ 391 nm is first generated by a vibrational Raman scattering of molecular ions, then the generated 391-nm coherent emission induces superfluorescence corresponding to the transition of $N_2^+(B^2\Sigma_u^+, v'=0) \rightarrow N_2^+(X^2\Sigma_g^+, v=0)$.

Figure 4 shows the Raman-scattering process under single photon resonant condition pumped by the 357-nm laser beam. In Fig. 4(a) the Stokes photons of 386 nm is generated through the vibrational Raman transition of $N_2^+(X^2\Sigma_g^+, v=0 \rightarrow v=1)$, and in Fig. 4(b) the Stokes photons of 391 nm is generated through the vibrational Raman transition of $N_2^+(B^2\Sigma_u^+, v'=0 \rightarrow v'=1)$. Because of the high population in $N_2^+(X^2\Sigma_g^+, v=0)$ and $N_2^+(B^2\Sigma_u^+, v'=0)$ [20,21], it is expected that the Raman scattering shown in Figs. 4(a) and 4(b) can occur simultaneously. However, the second harmonic of the 800-nm pump laser shown in Fig. 1(a) only covers the wavelength of 391 nm, which serves as the Stokes beam. The existence of the Stokes beam can greatly enhance the Raman process in Fig. 4(b)

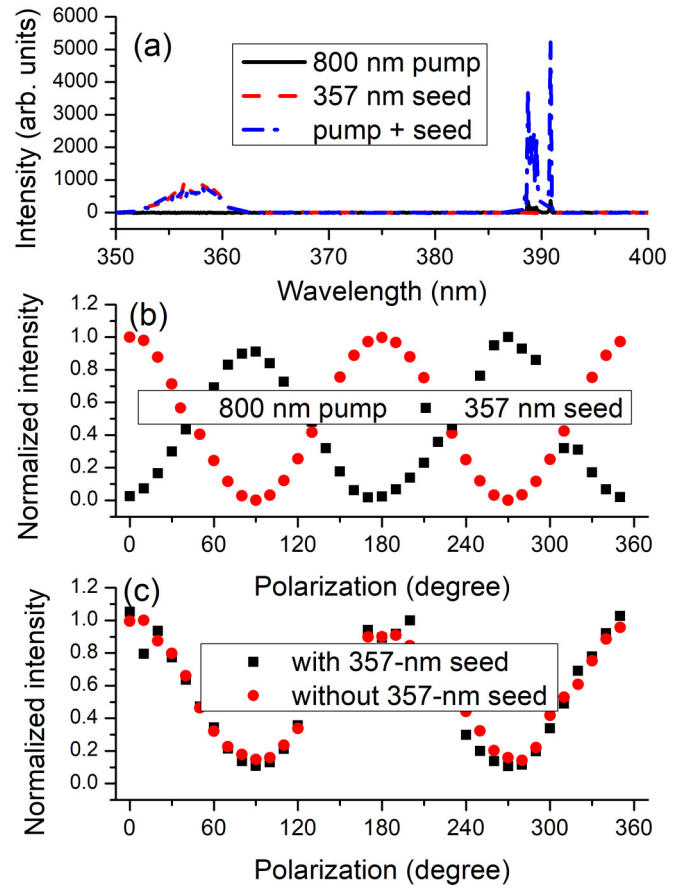


FIG. 5. (a) Forward emission in the presence of an external 357-nm seed with polarization perpendicular to the 800-nm pump laser polarization, (b) polarization properties of the 800-nm pump laser and 357-nm seed, (c) polarization properties of the 391-nm coherent emission with and without the 357-nm seed.

through stimulated-Raman scattering [39,40]. The stimulated-Raman-scattering process requires that the 357-nm seed and the second harmonic of the 800-nm pump laser overlaps in the temporal domain. This explains the observation shown in Fig. 2(a), wherein the enhancement only occurs within a limited temporal window near the duration of the 357-nm seed. The resonant stimulated-Raman scattering effectively converts coherent 357-nm photons into coherent 391-nm photons. In order to evaluate the conversion efficiency of the stimulated-Raman-scattering process, we measured the intensity of the 357-nm seed and the 391-nm seed under the condition that the same intensity is achieved for the enhanced 391-nm emission. The result indicates that about 2% of the 357-nm photons are converted into 391-nm photons through the resonant stimulated-Raman scattering.

Finally, we repeated the experiment using the 357-nm seed with polarization perpendicular to the 800-nm pump laser polarization. As depicted in Fig. 5(a), the 391-nm emission is also enhanced even though the enhancement degree is greatly decreased in comparison with the seed polarization parallel to the 800-nm pump laser polarization. Figure 5(b) shows the polarization of the 800-nm pump laser and the 357-nm seed, which are perpendicular to each other. Figure 5(c) show the polarization of the 391-nm coherent emission with

and without the 357-nm seed. It can be seen that the polarization of the 391-nm coherent emission is always parallel to the 800-nm pump laser polarization whether the 357-nm seed is applied or not. The observation that the polarization of the enhanced 391-nm emission is perpendicular to the polarization of the 357-nm seed is different from the case of the 391-nm seed, in which the polarization of the enhanced 391-nm emission is parallel to the polarization of the seed whether it is perpendicular or parallel [31]. In the following, we explore the mechanism behind this. As we discussed above, the enhanced 391-nm coherent emission is generated through two steps when the 357-nm seed is applied. In the first step, 357-nm coherent photons are converted into 391-nm coherent photons through stimulated-Raman scattering. As shown in Fig. 4(b), the conversion of the 357-nm photons into 391-nm photons is realized through the transition of $N_2^+(B^2\Sigma_u^+, v' = 1 \leftarrow X^2\Sigma_g^+, v = 0)$ and $N_2^+(B^2\Sigma_u^+, v' = 0 \rightarrow X^2\Sigma_g^+, v = 0)$. It should be emphasized that the dipole coupling between $N_2^+(B^2\Sigma_u^+)$ and $N_2^+(X^2\Sigma_g^+)$ becomes maximum when the laser polarization is parallel to the molecular axis [21]. In our experiment, ionized nitrogen molecules are generated through tunneling ionization. $N_2^+(B^2\Sigma_u^+)$ and $N_2^+(X^2\Sigma_g^+)$ are aligned along the polarization direction of the 800-nm pump laser at the moment of ionization due to the anisotropic angular-dependent ionization probability [37]. Here the second harmonic of the 800-nm pump laser serves as the Stokes beam and its polarization is confirmed to be parallel to the 800-nm pump laser polarization. Even though the initial polarization of the 357-nm seed is linearly polarized and perpendicular to the 800-nm pump laser polarization, the aligned molecules induced by the 800-nm pump laser will cause birefringence and

depolarize the 357-nm seed [41]. Thus, the generated parallel component is involved in the stimulated-Raman scattering to convert the 357-nm photons into 391-nm photons. Further, the generated 391-nm coherent emission serves as an external seed to induce superfluorescence from the ionized nitrogen molecules. As a result, the polarization of the superfluorescence has the same polarization of the 800-nm pump laser.

IV. SUMMARY

In summary, we report a phenomenon that a lagged coherent emission around 391 nm can be greatly enhanced when an external seed around 357 nm is injected into the ionized nitrogen molecules generated by the 800-nm laser fields. The enhanced 391-nm coherent emission is generated through a two-step process. In the first step, about 2% of the 357-nm coherent photons are converted into 391-nm coherent photons through stimulated vibrational Raman-scattering process. In the second step, the generated 391-nm coherent emission serves as an external seed to induce superfluorescence from the ionized nitrogen molecules. This study demonstrates that the seed wavelength can be different from the lasing wavelength, and our finding provides a different route to control the coherent emission from air filamentation induced by intense femtosecond laser fields.

ACKNOWLEDGMENTS

This work is supported by the National Key R&D Program of China (Grant No. 2018YFA0306302) and the National Natural Science Foundation of China (Grant Nos. 11625414, 21673006, 11474009, and 11434002).

-
- [1] J. Kasparian *et al.*, *Science* **301**, 61 (2003).
 [2] G. Sansone *et al.*, *Science* **314**, 443 (2006).
 [3] A. Y. Vorobyev, V. S. Makin, and C. Guo, *Phys. Rev. Lett.* **102**, 234301 (2009).
 [4] J. Yao, B. Zeng, H. Xu, G. Li, W. Chu, J. Ni, H. Zhang, S. L. Chin, Y. Cheng, and Z. Xu, *Phys. Rev. A* **84**, 051802 (2011).
 [5] Q. Luo, W. Liu, and S. L. Chin, *Appl. Phys. B* **76**, 337 (2003).
 [6] A. Dogariu, J. B. Michael, M. O. Scully, and R. B. Miles, *Science* **331**, 442 (2011).
 [7] D. Kartashov, S. Ališauskas, G. Andriukaitis, A. Pugžlys, M. Shneider, A. Zheltikov, S. L. Chin, and A. Baltuška, *Phys. Rev. A* **86**, 033831 (2012).
 [8] A. Laurain, M. Scheller, and P. Polynkin, *Phys. Rev. Lett.* **113**, 253901 (2014).
 [9] S. Mitryukovskiy, Y. Liu, P. Ding, A. Houard, and A. Mysyrowicz, *Opt. Express* **22**, 12750 (2014).
 [10] A. J. Traverso, R. Sanchez-Gonzalez, L. Yuan, K. Wang, D. V. Voronine, A. M. Zheltikov, Y. Rostovtsev, V. A. Sautenkov, A. V. Sokolov, S. W. North, and M. O. Scully, *Proc. Natl. Acad. Sci. USA* **109**, 15185 (2012).
 [11] P. N. Malevich, R. Maurer, D. Kartashov, S. Ališauskas, A. A. Lanin, A. M. Zheltikov, M. Marangoni, G. Cerullo, A. Baltuška, and A. Pugžlys, *Opt. Lett.* **40**, 2469 (2015).
 [12] K. Yamanouchi, *Science* **295**, 1659 (2002).
 [13] X. M. Tong, Z. X. Zhao, and C. D. Lin, *Phys. Rev. A* **66**, 033402 (2002).
 [14] B. K. McFarland, J. P. Farrell, P. H. Bucksbaum, and M. Gühr, *Science* **322**, 1232 (2008).
 [15] O. Smirnova, Y. Mairesse, S. Patchkovskii, N. Dudovich, D. Villeneuve, P. Corkum, and M. Y. Ivanov, *Nature (London)* **460**, 972 (2009).
 [16] H. Akagi, T. Otobe, A. Staudte, A. Shiner, F. Turner, R. Dörner, D. M. Villeneuve, and P. B. Corkum, *Science* **325**, 1364 (2009).
 [17] C. Wu, H. Zhang, H. Yang, Q. Gong, D. Song, and H. Su, *Phys. Rev. A* **83**, 033410 (2011).
 [18] J. Yao, G. Li, X. Jia, X. Hao, B. Zeng, C. Jing, W. Chu, J. Ni, H. Zhang, H. Xie, C. Zhang, Z. Zhao, J. Chen, X. Liu, Y. Cheng, and Z. Xu, *Phys. Rev. Lett.* **111**, 133001 (2013).
 [19] Y. Liu, P. Ding, G. Lambert, A. Houard, V. Tikhonchuk, and A. Mysyrowicz, *Phys. Rev. Lett.* **115**, 133203 (2015).
 [20] H. Xu, E. Lötstedt, A. Iwasaki, and K. Yamanouchi, *Nat. Commun.* **6**, 8347 (2015).
 [21] J. Yao, S. Jiang, W. Chu, B. Zeng, C. Wu, R. Lu, Z. Li, H. Xie, G. Li, C. Yu, Z. Wang, H. Jiang, Q. Gong, and Y. Cheng, *Phys. Rev. Lett.* **116**, 143007 (2016).
 [22] M. Lei, C. Wu, A. Zhang, Q. Gong, and H. Jiang, *Opt. Express* **25**, 4535 (2017).

- [23] Z. Liu, J. Yao, J. Chen, B. Xu, W. Chu, and Y. Cheng, *Phys. Rev. Lett.* **120**, 083205 (2018).
- [24] J. Yao, W. Chu, Z. Liu, B. Xu, J. Chen, and Y. Cheng, *New J. Phys.* **20**, 033035 (2018).
- [25] H. Xu, E. Lotstedt, T. Ando, A. Iwasaki, and K. Yamanouchi, *Phys. Rev. A* **96**, 041401 (2017).
- [26] A. Azarm, P. Corkum, and P. Polynkin, *Phys. Rev. A* **96**, 051401(R) (2017).
- [27] X. Zhong, Z. Miao, L. Zhang, Q. Liang, M. Lei, H. Jiang, Y. Liu, Q. Gong, and C. Wu, *Phys. Rev. A* **96**, 043422 (2017).
- [28] Y. Liu *et al.*, *Phys. Rev. Lett.* **119**, 203205 (2017).
- [29] M. Britton, P. Laferrière, D. H. Ko, Z. Li, F. Kong, G. Brown, A. Naumov, C. Zhang, L. Arissian, and P. B. Corkum, *Phys. Rev. Lett.* **120**, 133208 (2018).
- [30] L. Arissian, B. Kamer, A. Rastegari, and D. Villeneuve, [arXiv:1802.00063](https://arxiv.org/abs/1802.00063).
- [31] H. Zhang, C. Jing, J. Yao, G. Li, B. Zeng, W. Chu, J. Ni, H. Xie, H. Xu, S. L. Chin, K. Yamanouchi, Y. Cheng, and Z. Xu, *Phys. Rev. X* **3**, 041009 (2013).
- [32] X. Liu, D. Umstadter, E. Esarey, and A. Ting, *IEEE Trans. Plasma Sci.* **21**, 90 (1993).
- [33] Y. Liu, Y. Brelet, G. Point, A. Houard, and A. Mysyrowicz, *Opt. Express* **21**, 22791 (2013).
- [34] X. Zhong, Z. Miao, L. Zhang, H. Jiang, Y. Liu, Q. Gong, and C. Wu, *Phys. Rev. A* **97**, 033409 (2018).
- [35] G. Li, C. Jing, B. Zeng, H. Xie, J. Yao, W. Chu, J. Ni, H. Zhang, H. Xu, Y. Cheng, and Z. Xu, *Phys. Rev. A* **89**, 033833 (2014).
- [36] M. Nagasono, J. R. Harries, H. Iwayama, T. Togashi, K. Tono, M. Yabashi, Y. Senba, H. Ohashi, T. Ishikawa, and E. Shigemasa, *Phys. Rev. Lett.* **107**, 193603 (2011).
- [37] S. Petretti, Y. V. Vanne, A. Saenz, A. Castro, and P. Decleva, *Phys. Rev. Lett.* **104**, 223001 (2010).
- [38] A. Mysyrowicz *et al.*, [arXiv:1806.05818](https://arxiv.org/abs/1806.05818).
- [39] R. C. Prince, R. R. Frontiera, and E. O. Potma, *Chem. Rev.* **117**, 5070 (2017).
- [40] D. Kim, D. S. Choi, J. Kwon, S.-H. Shim, H. Rhee, and M. Cho, *J. Phys. Chem. Lett.* **8**, 6118 (2017).
- [41] J. Huang, C. Wu, N. Xu, Q. Liang, Z. Wu, H. Yang, and Q. Gong, *J. Phys. Chem. A* **110**, 10179 (2006).